

Electronic Supplementary Information (ESI)

Role of gas-phase dynamics on interfacial phenomena during few-layer graphene growth through atmospheric pressure chemical vapour deposition

Fatin Bazilah Fauzi^a, Edhuan Ismail^a, Syed Noh Syed Abu Bakar^b, Ahmad Faris Ismail^b, Mohd Ambri Mohamed^c, Muhamad Faiz Md Din^d, Suhaimi Illias^e, and Mohd Hanafi Ani^{a*}

^a*Department of Manufacturing and Materials, Kulliyah of Engineering, International Islamic University Malaysia, P.O. Box 10, 50728 Kuala Lumpur, Malaysia*

^b*Department of Mechanical, Kulliyah of Engineering, International Islamic University Malaysia, P.O. Box 10, 50728 Kuala Lumpur, Malaysia*

^c*Institute of Microengineering and Nanoelectronics, Universiti Kebangsaan Malaysia, 43600 Bangi, Malaysia*

^d*Department of Electrical and Electronics Engineering, Level 7, Bestari Block, Universiti Pertahanan Nasional Malaysia, Sungai Besi Camp, 57000 Kuala Lumpur, Malaysia*

^e*School of Manufacturing Engineering, Universiti Malaysia Perlis, Kampus Alam Pauh Putra, 02600 Arau, Perlis, Malaysia*

Email: mhanafi@iium.edu.my

Table S1 Various gas flow composition for APCVD of graphene using a Cu catalyst.

Total flowrate (sccm)	0.01 CH₄ (sccm)	0.05 H₂ (sccm)	0.94 Ar (sccm)
100 - 1000	1 - 10	5 - 50	94 - 940

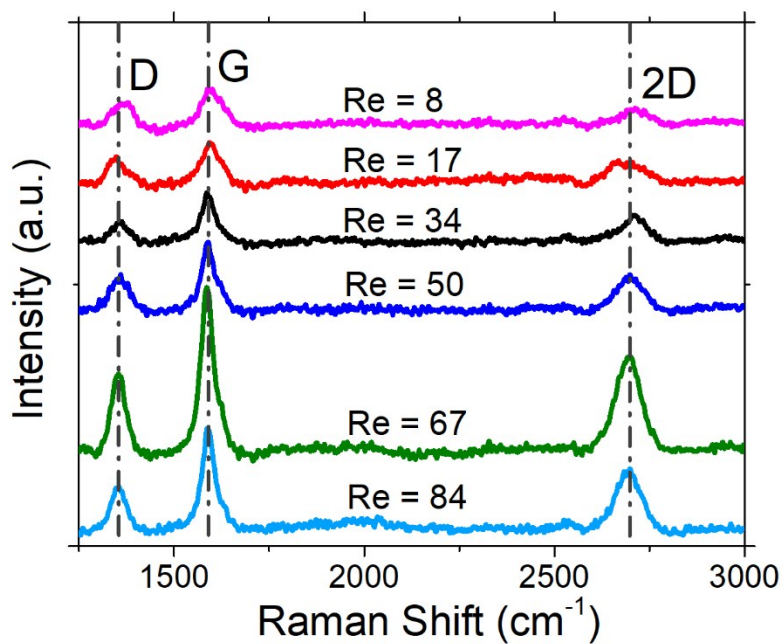


Figure S1 Raman spectra of the graphene deposited at different Reynolds number varies from 8 to 84 with D, G and 2D peaks.

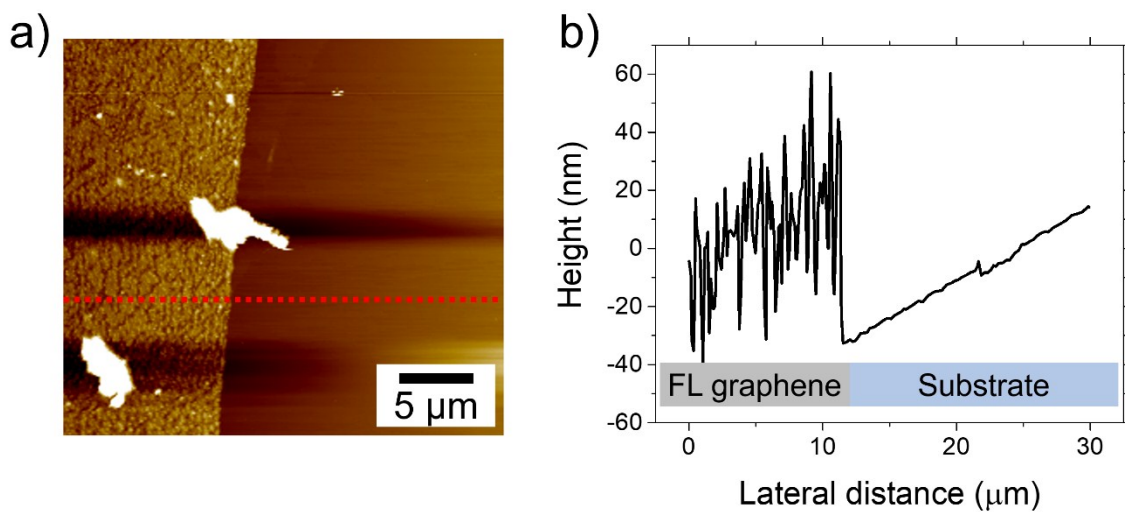


Figure S2 a) AFM image of deposited graphene flake on quartz substrate and b) height profile of the graphene flake along the red dotted line in (a).

Calculations on mass transport, residence time and diffusion time

For these calculations, few assumptions are made. First, the gas mixture obeys the ideal gas law. Second, CH₄ was the only diffused species considered because the exact species responsible for graphene deposition is still not conclusively identified¹. Third, the boundary layer thickness used in the calculation is the velocity boundary layer thickness. Here, the thermal boundary layer and the concentration boundary layer can be used to achieve the same effect². Fourth, we used the Grove stagnant-film model. In this model, the boundary layer is a stagnant film of thickness formed on the solid surface due to the steady state of the gas flow³.

Following the Fick's law of diffusion, the diffusion flux, F_1 from the bulk gas towards the surface is:

$$F_1 = h_G(C_G - C_S) \quad (S1)$$

where h_G is the mass transport coefficient, C_G and C_S are the concentration at the bulk and on the surface respectively. The concentration is substituted with P_i/RT according to ideal gas law equation⁴ then equivalently expressed by:

$$F_1 = h_G \frac{(P_G - P_S)}{RT} \quad (S2)$$

where P_G and P_S are the partial pressure at the bulk gas and on the surface respectively, R is the gas constant and T is the temperature. In a steady state, diffusion flux is equal to the deposition flux, F_2 ($F_1 = F_2$)⁵. For a mass transport controlled condition, the deposition rate, R_D is:

$$R_D = h_G \frac{(P_G - P_S)M_{CH_4}}{RT} \quad (S3)$$

where M_{CH_4} is the molecular weight of methane. Based on the Grove stagnant-film model, mass transport coefficient can be calculated using the equation:

$$h_G = \frac{D_{CH_4}}{\delta} \quad (S4)$$

where D_{CH_4} is the diffusion coefficient and δ is the boundary layer thickness. Diffusion coefficient of CH₄ in hydrogen and argon mixture is calculated using the Maxwell-Stefan equation:

$$D_{CH_4} = \frac{1 - Y_1}{Y_2/D_{12} + Y_3/D_{13}} \quad (S5)$$

Where Y_1 , Y_2 , Y_3 are the molar fraction of each component and D_{12} , D_{13} are the diffusion coefficients in 12 and 13 binary systems, respectively (1-CH₄; 2-H₂; 3-Ar). The diffusion coefficient of the binary system estimated using Chapman-Enskog theory where the average

$$D_{12} = \frac{1.86 \times 10^{-3} T^{3/2} \left(\frac{1}{M_1} + \frac{1}{M_2}\right)^{1/2}}{p \sigma_{12}^2 \Omega} \quad (S6)$$

accuracy prediction is within 8% ⁶:

Where T is the absolute temperature, M_1 , M_2 are the molecular weights, p is the pressure, σ and Ω are the molecular properties characteristics. The average collision diameter, σ_{12} obtained from $\sigma_{12} = 1/2 (\sigma_1 + \sigma_2)$ while the dimensionless quantity of collision integral, Ω can be found as a function of $\kappa_B T / \varepsilon_{12}$ where the energy of the interaction of ε_{12} is $\varepsilon_{12} / \kappa_B = \sqrt{\varepsilon_1 / \kappa_B \cdot \varepsilon_2 / \kappa_B}$. Individual values of σ and ε listed in the table of Lennard-Jones potential parameters were found from viscosities ⁷.

The residence time is calculated using Eq. S7:

$$t_r = \frac{V_r}{Q^0 \times \left(\frac{T}{T^0}\right) \times \left(\frac{P^0}{P}\right)} \quad (S7)$$

Where V_r is the hot-zone volume ($V_r = \pi r^2 L$), Q^0 is the volumetric flow rate for standard temperature and pressure (STP) in standard cubic cm per min (sccm), whereas T and P are mean absolute temperature and pressure respectively.

$$t \approx \frac{\delta^2}{D_{CH_4}} \quad (S8)$$

While diffusion time is calculated using Eq. S8 ⁸.

References

- 1 P. Li, Z. Li and J. Yang, *J. Phys. Chem. C*, 2017, **121**, 25949–25955.
- 2 Y. Xu and X.-T. Yan, *Chemical Vapour Deposition An Integrated Engineering Design for Advanced Materials*, Springer Heidelberg Dordrecht London New York, London, 2010.
- 3 A. S. Grove and J. Wiley, *Physics and Technology of Semiconductor Devices*, John Wiley & Sons, Inc, 1967.
- 4 M. Ohring, *Materials Science of Thin Films*, Elsevier, Second Edi., 2002.
- 5 C. R. Å. Kleijn, R. Dorsman, K. J. Kuijlaars, M. Okkerse and H. Van Santen, 2007, **303**, 362–380.
- 6 B. E. Poling, J. M. Prausnitz and J. P. O’Connell, *The properties of gases and liquids*, McGraw-Hill Professional, Fifth edit., 2000.
- 7 E. L. Cussler, *Diffusion Mass Transfer in Fluid Systems*, Cambridge University Press, Third Edit., 2009.
- 8 O. Feron, F. Langlais, R. Naslain and J. Thebault, *Carbon N. Y.*, 1999, **37**, 1343–1353.